

Anticorrosive Effects of Leek Seeds Aqueous Extract (*Allium ampeloprasum* Var. Kurrat) on Aluminum Alloys 6061, 7075 and 2024 in Seawater



Aisha H Al-Moubaraki* and Hind H Al-Rushud

Department of chemistry, Alfaisaliah Campus, Saudi Arabia

Submission: September 16, 2017; Published: September 25, 2017

*Corresponding author: Aisha H Al-Moubaraki, Department of Chemistry, Faculty of Sciences, Alfaisaliah Campus, King Abdulaziz University, Jeddah, Saudi Arabia, Email: ahm13988@hotmail.com, ahmubarakikau.edu.sa

Abstract

The anticorrosive effects of Leek seeds aqueous extract (LSAE), *Allium ampeloprasum* var. *kurrat*, on Al 6061, Al 7075, and Al 2024 in seawater was investigated using weight loss (WL) measurements and potentiodynamic polarization (PDP) technique. The effectiveness of the inhibitor was studied as a function of temperature using PDP technique. The results showed that LSAE can work as effective corrosion inhibitor and inhibition efficiencies increased with the increase of LSAE concentration. The inhibition efficiency of Al 6061 improved with an increase in temperature, whereas the inhibition efficiency of Al 7075 and Al 2024 was decreased with an increase in temperature. Adsorption of organic molecules on alloys surfaces was emphasized by energy-dispersive X-ray spectroscopy (EDS). Temkin Adsorption isotherm was found to be the best fit for the experimental polarization data and adsorption strengths of the LSAE molecules on the studied alloys surfaces increased as follows: Al 6061 > Al 7075 > Al 2024.

Keywords: Seawater; Corrosion; Al alloys; Inhibition; Polarization; Adsorption; Leek seeds

Abbreviations: LSAE: Leek Seeds Aqueous Extract; PDP: Potentiodynamic Polarization; WL: Weight Loss; EDS: Energy Dispersive X-ray Spectroscopy; IGC: Inter Granular cracking

Introduction

Aluminum is the second most used metal and more than several dozens of aluminum alloys are used in different areas of manufacturing and technology [1,2]. Aluminum resists uniform corrosion under natural conditions due to formation of adherent passive oxide film on its surface, but presence of aggressive anions in the environment like chloride ions in seawater can weaken the passive oxide film [3-5]. Aluminum alloys are prone to localized corrosion in chloride environment as pitting, crevice and intergranular corrosion [6,7]. The micro galvanic coupling between alloys matrix and the intermetallic particles results in pitting corrosion and further develop intergranular cracking (IGC) into the deep structure of Al alloys [8]. Cu-containing intermetallic particles play an important role in the corrosion of high strength aluminum alloys; they can act as cathodes with respect to the matrix and support oxygen reduction [8,9].

The use of inhibitors is one of the most important and economical ways to protect metal or alloys surfaces against corrosion [10]. Corrosion inhibitor is any chemical additive

which when added in small concentrations to an environment increase the corrosion resistance [11,12]. The protective action of the inhibitors can be achieved through different mechanisms. Organic inhibitors mostly are adsorbed on the metal surfaces and form a protective layer. On other hand, inorganic inhibitors tend to form oxide film or hardly soluble salt on the metal surface. Some inhibitors can react with aggressive components present in aqueous medium and make the environment less corrosive [11,13].

Despite the excellent inhibitive properties of large number of organic, inorganic and polymeric compounds proved in previous studies, most of them are toxic and biodegradable which can cause jeopardizing effects to marine life. Because of increasing concern about the toxicity and biodegradability of corrosion inhibitors discharged into the environment, Scientific community has been focused toward the development of friendly environmentally inhibitors [14-16]. Plant extracts have been reported widely in literature as effective and environmentally acceptable corrosion inhibitors in different aggressive environments [16,17].

The plant extracts (dried stem, seeds, leaves and fruits) comprise organic compounds containing hetero atoms with lone pair of electrons, π bonds, triple bonds and heterocyclic compounds. They don't contain heavy metals or toxic compounds. Inhibition efficiency of plant extracts is usually due to adsorption of these organic compounds over the metal surface via hetero atoms containing lone pair (N, O and S) or via π -electrons [16]. Rosliza and Izman [18] studied the corrosion protections and the mechanism of corrosion inhibitions of natural products (natural honey, vanillin, and tapioca starch) for an Al-Mg-Si alloy in seawater at room temperature using SEM and EDS characterization and the results revealed that the natural products effectively inhibited the corrosion products on the alloy surface and protected the passive film from dissolution in seawater.

Allium ampeloprasum var. Kurrat is the Middle East cultivated leek. It is a popular leafy vegetable [19,20]. It has been considered as one of the popular medicine. Its medicinal property is mainly due to the presence of many sulphur containing bio-active constituents as dimethyl disulfide, methyl propenyl disulfide, propyl propenyl disulfide, etc. leek also contains higher amount of methiin and propiin, which is responsible for its odors and considered to be beneficial to health [20]. There is no information available for the anticorrosive properties of leek on aluminum or its alloys. Thus we choose leek seeds to study its inhibitive effect on aluminum alloys in seawater. The present work aims to investigate the anticorrosive properties of leek seeds aqueous extract (LSAE) on three different aluminum alloys (Al 6061, Al7075, and Al 2024) in seawater using weight loss (WL) measurements and potentiodynamic polarization (PDP)

Table 1: Percentage composition of the studied Al alloys.

Alloy	Cr	Cu	Fe	Mg	Mn	Si	Ti	Zn	Zr	Al
7075	0.18-0.28	1.2-2	0.5	2.1-2.9	0.3	0.4	0.2	5.1-6.1	0.25	Remainder
2024	0.1	3.8-4.9	0.5	1.2-1.8	0.3-0.9	0.5	0.15	0.25	-	Remainder
6061	0.04-0.35	0.15-0.4	0.7	0.8-1.2	0.15	0.4-0.8	0.15	0.25	-	Remainder

C) Test Solution: The test solution was natural seawater and it was collected directly from the Red Sea in the western region (Obhur, Jeddah, Saudi Arabia). Numerous properties of the sample such as pH, electrical conductivity, total alkalinity and content of different ions were illustrated in previous work [21].

Techniques

A) Weight Loss (WL) Measurement: Polished and pre-weighed Al specimens were placed in airtight glass containers containing seawater without and with different concentration of LSAE (0.1-1.5 g of LSAE/L of seawater). The containers closed and left at room temperature for five weeks. At the end of immersion period, the specimens were assessed by weight-loss measurement after corrosion products were removed by pickling in concentrated nitric acid for 1-5 minutes, ASTM G1 [22]. Visual photographs were taken of the samples with an optical camera to evaluate changes in the alloys surfaces. The percentage of

technique. Aluminum alloys surfaces were detected using visual photographs and electron-dispersive energy spectroscopy (EDS). Effect of temperature on adsorption and inhibition efficiencies was studied and the thermodynamic parameters were calculated and discussed.

Experimental

Materials

A) Leek Seed Aqueous Extract (LSAE): Leek seed aqueous extract was prepared by heating 10 g of the seeds in 100 mL of distilled water for 2 hours. After that the solution was allowed to cool at room temperature, filtered, then poured in a Pyrex tray and evaporated at 60°C for 24 hours using hot air oven. The resultant powders were collected and stored in a desiccator to be used as a natural inhibitor. The structure of the inhibitor was investigated by IR spectroscopy. Inhibition solutions were prepared by mixing (0.1-1.5)g of the inhibitor /L of seawater.

B) Specimens and Surface Pretreatment: Three different types of commercial aluminum alloys (Al 6061, Al 2024 and Al 7075) were used in this research. The chemical composition of the studied Al alloys was presented in (Table 1). Specimens, 10 to 15 mm in diameter and 40 to 50 mm in length were cut from the respective metal rods. Before each experiment, the specimens were mechanically abraded using emery papers (80-1200 grades), washed with distilled water, degreased in ethanol and then dried using a stream of air. The specimens finally were weighed accurately and immersed in the test solution.

inhibition efficiency obtained from weight loss measurements can be calculated as:

$$\%IE_{WL} = \frac{\Delta W^o - \Delta W}{\Delta W} \times 100 \quad (1)$$

Where ΔW^o and ΔW represent the weight loss of Al alloys without and with of certain concentration of LSAE, respectively.

B) Potentiodynamic Polarization (PDP) Technique: Potentiodynamic polarization measurements were performed by connecting the electrochemical cell to **ACM Gill AC potentiostat / galvanostat 1649**. The electrochemical cell consists of working electrode (Al 6061, Al 2024 and Al 7075 used as working electrodes), a reference electrode (Ag/AgCl(s)/KCl_{saturated}(aq)) and a platinum counter electrode. Prior to each experiment, working electrode was abraded and treated as referred in section(B), then immersed in seawater without and with different concentration of the inhibitor and allowed to stabilize for 2 hours. Polarization curves were recorded by changing the electrode potential automatically from -1200 to -200 mV at a

constant sweep rate of **1 mV/sec**. Corrosion current density (i_{corr}) can be obtained from extrapolation the linear portion of either measured anodic or cathodic curves and intersecting these extrapolated lines with a line drawn from (E_{corr}) [23-25].

As the rate of oxidation is equal the rate of reduction at E_{corr} , the extrapolations of both anodic and cathodic linear Tafel regions must intersect at E_{corr} . If this does not occur, there is an error in the measurement. The error is probably in the anodic measurement. Since the surface is changing because of corrosion and/or passivation of the metal or alloy. If this behavior is observed, it is probably safest to measure corrosion current density at the point where the cathodic Tafel extrapolation intersects E_{corr} [24,26]. Because of that corrosion current densities were obtained from polarization curves by extrapolation cathodic Tafel line to corrosion potential using ACM Gill software. The percentage inhibition efficiency can be obtained from potentiodynamic polarization measurements as follows:

$$IE_i \% = \left(1 - \frac{i_{corr}}{i_{corr}^0}\right) \times 100 \quad (2)$$

Where i_{corr} and i_{corr}^0 are the corrosion current densities without and with of certain concentration of LSAE, respectively.

C) Energy-Dispersive X-ray Spectroscopy (EDS): The energy-dispersive X-ray spectroscopy (EDS) was used to analyze the elements on the surfaces of alloys after immersion in seawater for five weeks without and with specific concentration of LSAE.

D) Fourier Transform Infrared Analysis (FTIR): FTIR spectra were recorded using a Perkin-Elmer spectrophotometer model Frontier (USA), which extended from 400 to 4000 cm^{-1} using the KBr disk technique. The sample of FTIR characterization is the LSAE powder, which was mixed with KBr and compressed as a disk. An infrared light was passing through the sample. The spectrometer was used to identify the functional groups of LSAE by observing at the vibrational motion of bonds in the molecules.

Results and Discussion

Effect of Inhibitor Concentration

Table 2: Inhibition efficiencies of A1 6061, A1 7075, and A1 2024 in seawater with different concentration of LSAE at 25°C.

C_{inh} (g/L)	Inhibition Efficiency (IE_{WL} %)		
	Al 6061	Al 7075	Al 2024
0.10	74.46	- 37.50	- 68.00
0.25	78.72	57.50	- 57.33
0.50	82.97	75.00	47.50
0.75	91.48	90.00	78.60
1.00	95.74	91.25	86.60
1.50	97.87	95.00	92.00

Weight Loss (WL): Table 2 shows the inhibition efficiency of Al 6061, Al 2024 and Al 7075 as a function of different concentrations of the inhibitor in seawater. The data in Table 2 shows that the inhibition efficiency increased for all the alloys with increase in inhibitor concentration, as a result of that, the inhibitor concentrations enhanced the adsorption of the inhibitor on alloys surfaces which resulted in more reduction in corrosion rate and increase in the inhibition efficiency. Adding a low concentration (0.1 g/L) of the inhibitor reduced the corrosion rate of Al 6061 by 74.46% efficiency, while the corrosion rates of the other alloys increased with low concentration (0.1 for Al 7075 and 0.1-0.25 for Al 2024).

The acceleration of corrosion is greater at lower concentrations and is found to decrease with increase in extract concentrations. The acceleration by LSAE in seawater may be attributed to the following factors:

- the lowering of over potential for the cathodic process (oxygen reduction);
- catalytic action of the adsorbed species on the reduction of oxygen; and
- The formation of readily soluble complexes which lower the over potential of the cathodic process [27]. Cathodic stimulation may be caused by the ability of organic species to produce a catalytic path of lowered activation energy for oxygen reduction [28]. At one and the same concentration of LSAE, the inhibition efficiency of LSAE for the studied Al alloys follows the order is given below:

Al 6061 > Al 7075 > Al 2024

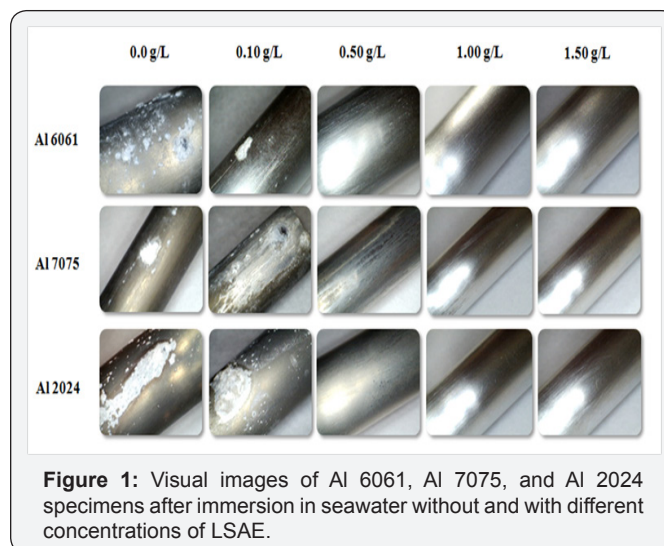


Figure 1: Visual images of Al 6061, Al 7075, and Al 2024 specimens after immersion in seawater without and with different concentrations of LSAE.

This order is contrary to the numbers of cathodic Cu-containing IM particles present on the alloys surfaces as reported in previous study [9], (Al 2024 > Al 7075 > Al 6061). Cu-rich intermetallic particles enhance corrosion by acting as a cathode [8,9] thus more cathodic particles present on alloys surfaces increased the area that are susceptible to corrosion

which required higher concentration of the inhibitor to protect the alloys against corrosion. (Figure 1) shows images of Al 6061, Al 2024 and Al7075 after five weeks of immersion in seawater with different concentrations of the inhibitor. With high concentration, no pitting was observed and the corrosion products disappeared. These results proved that LSAE effectively protected Al alloys and suppressed the corrosion process.

Potentiodynamic Polarization (PDP)

Table 3: Polarization parameters of A1 6061, A1 7075, and A1 2024 immersed in seawater without and with different concentrations of LSAE at 25°C.

Cinh(g/L)	E_{corr} (mV)	i_{corr} ($\mu\text{A}/\text{cm}^2$)	$-b_c$ (mV/dec)	$IE_i\%$
Al 6061				
0.00	-814	1.38	222	0
0.25	-712	0.48	180	65
0.50	-829	0.39	166	71
0.75	-807	0.36	167	74
1.50	-728	0.27	228	81
Al 7075				
0.00	-732	5.78	351	0
0.25	-730	3.39	240	41
0.50	-756	2.74	179	52
0.75	-758	2.05	176	61
1.00	-732	1.81	162	69
Al 2024				
0.00	-842	3.20	167	0
0.50	-820	2.69	170	16
0.75	-824	1.98	150	38
1.00	-795	1.33	155	58
1.50	-797	0.89	144	72

The cathodic and anodic potentiodynamic polarization curves of aluminum alloys in seawater without and with different concentrations of LSAE for 2 hours are shown in (Figure 2). The electrochemical kinetic parameters (E_{corr} , i_{corr} , b_c) and the inhibition efficiency ($IE_i\%$) values are reported in (Table 3). Corrosion potential values (E_{corr}) of Al 2024 and Al 6061 shifted in the positive direction relative to the corrosion potential of free solution (without inhibitor), except Al 6061 at 0.5 g/L concentration, which exhibited small shift in the negative direction. Since both anodic and cathodic curves of Al 2024 and Al 6061 are affected, the inhibitor acted as a mixed-type inhibitor with predominantly anodic inhibition activities. In the case of Al 7075, corrosion potentials at different concentrations did not follow a definite pattern, E_{corr} values of two concentrations (0.5 and 0.75 g/L) were more slightly shifted towards cathodic potential but for the other two concentrations (0.25 and 1 g/L), corrosion potentials were almost equal to that of the free solution.

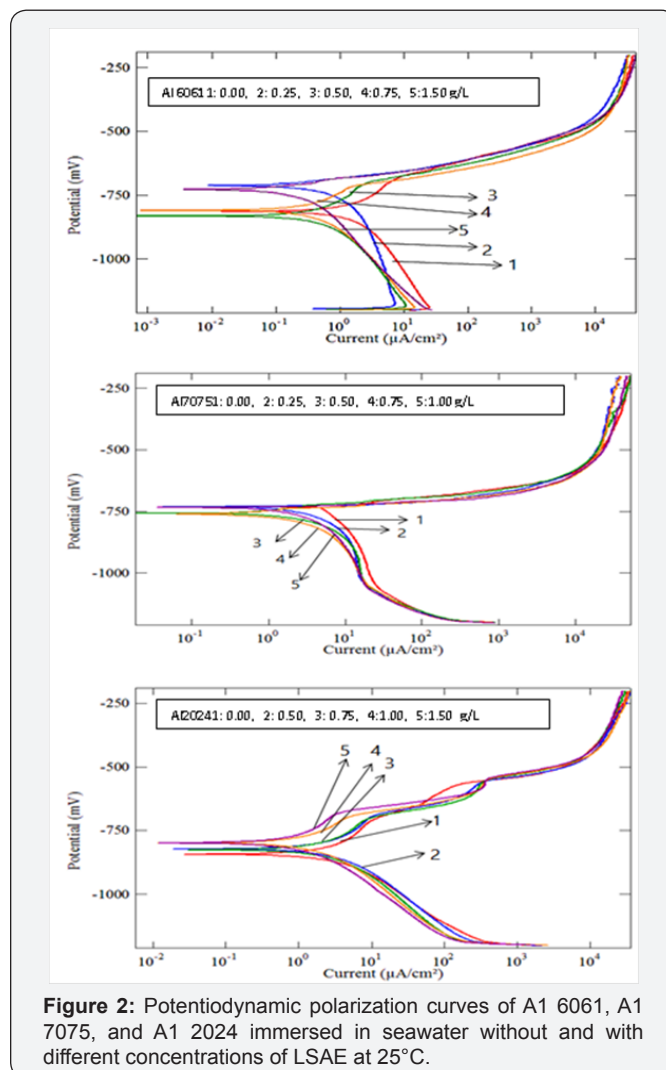


Figure 2: Potentiodynamic polarization curves of Al 6061, Al 7075, and Al 2024 immersed in seawater without and with different concentrations of LSAE at 25°C.

So, it is suggested that polarization curves of Al 7075 show mixed-type effect for the inhibition process. In previous study, Roliza et al. [29] reported that vanillin which is safe and high soluble in water was a mixed-type inhibitor for the corrosion of aluminum in seawater. Corrosion current density (i_{corr}) decreases with increasing inhibitor concentration which leads to an increase in inhibition efficiency ($IE_i\%$). At one and the same concentration of LSAE, the inhibition efficiency of LSAE for the studied Al alloys follows the order is given below:

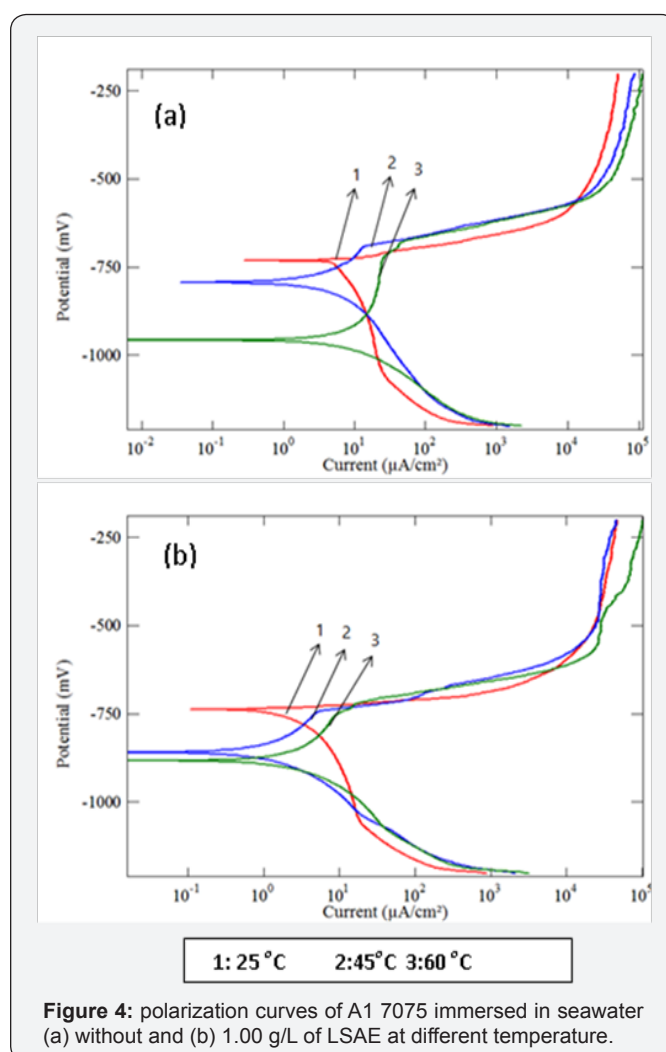
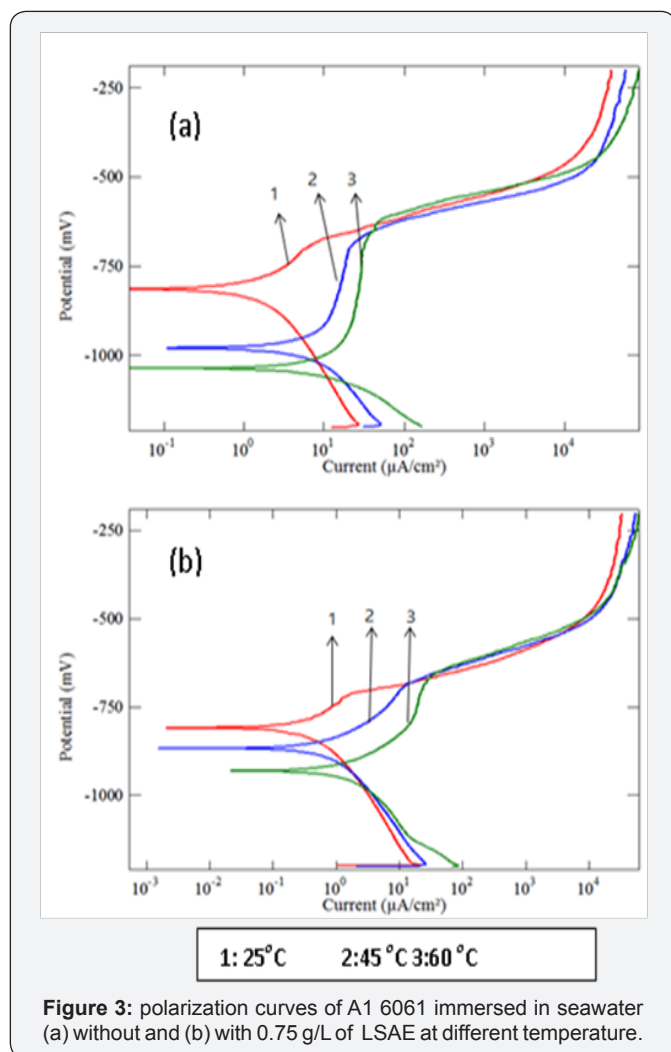
Al 6061 > Al 7075 > Al 2024.

Which is in agreement with that obtained from WL measurements? It is worth noting from Tables 2 & 3 that the inhibition efficiency values computed using PDP results are less than the values calculated from the WL method. This difference in inhibition efficiency values between WL and PDP may be attributed to a long-term prediction of corrosion inhibition can be achieved in the case of WL comparing to the less-time consuming electrochemical techniques of PDP. The results obtained from PDP and WL methods indicate that LSAE can work as an effective corrosion inhibitor for Al alloys in seawater.

Effect of Temperature on the Inhibition Efficiency

Table 4: Polarization parameters of A1 6061, A1 7075, and A1 2024 immersed in seawater without and with of LSAE at different temperature.

T (o C)	C_{inh} (g/L)	$-E_{corr}$ (mV)	$-b_c$ (mV / dec)	i_{corr} (μ A/cm ²)	C_{inh} (g/L)	$-E_{corr}$ (mV)	$-b_c$ (mV / dec)	i_{corr} (μ A/cm ²)	IE_i %
Al 6061									
25	0	814	222	1.38	0.75	807	167	0.36	74
45		978	176	5.38		866	214	0.89	83
60		1053	109	8.59		929	156	1.36	84
Al 7075									
25	0	732	351	5.78	1	732	162	1.81	69
45		793	276	6.71		858	193	2.31	65
60		956	132	9.49		883	184	4.37	53
Al 2024									
25	0	842	167	3.2	1.5	797	144	0.89	72
45		909	127	6.32		872	150	3.12	54
60		968	110	13.96		860	176	6.86	47



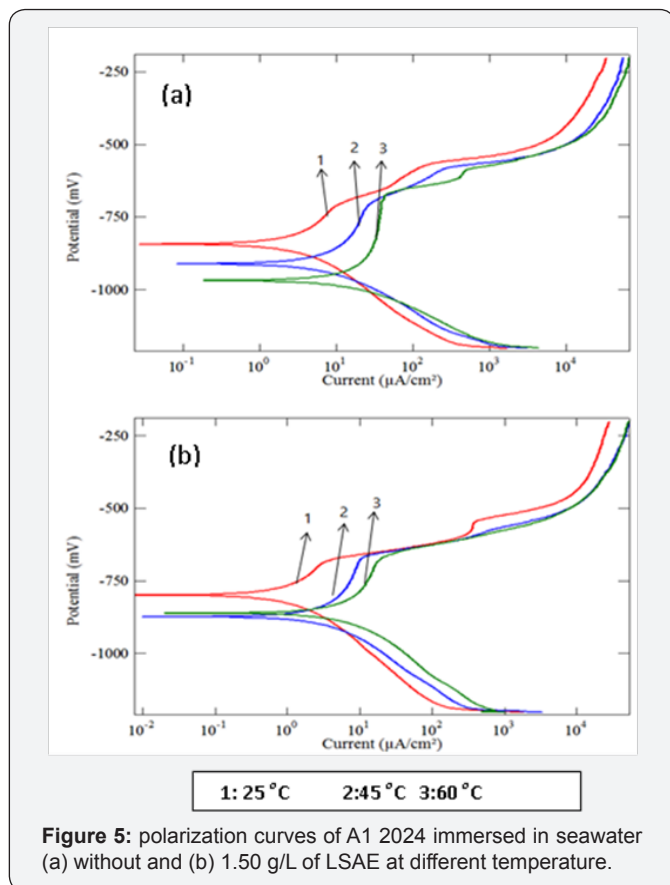


Figure 5: polarization curves of Al 2024 immersed in seawater (a) without and (b) 1.50 g/L of LSAE at different temperature.

The cathodic and anodic potentiodynamic polarization curves of aluminum alloys in seawater without and with specific concentration of LSAE (Al 6061 in 0.75 g/L, Al 7075 in 1.00 g/L and Al 2024 in 1.5 g/L) were measured at different temperatures (25°C, 45°C and 60°C) as shown in (Figures 3-5). The electrochemical parameters and inhibition efficiency of the studied alloys are given in (Table 4). The results of all the alloys show that increase in temperature resulted in an increase in corrosion current density (i_{corr}) and shifted the corrosion potential (E_{corr}) towards more negative values either in uninhibited or inhibited seawater. In general, a more negative corrosion potential indicates a more active state. The electrode became more vulnerable to the test solution with the increased temperature, which is associated with a higher anodic dissolution trend. Apparently, the increase in temperature significantly activated the Al alloys. The values of b_c for Al 6061, Al 7075, and Al 2024, respectively decreased significantly with temperatures. It indicated that the cathodic reaction was accelerated with temperature rising. It is well known that the cathodic reaction is a purely diffusion-controlled process within a certain potential region in aerated solutions [30].

It is dominated by the diffusion and the reduction of dissolved oxygen. With temperature rising, the coefficient of diffusion oxygen molecules increases which resulted in the acceleration of oxygen diffusion and thus the increase of cathodic reductive current density. The inhibition efficiency of

Al 6061 improved with an increase in temperature, whereas the inhibition efficiency of Al 2024 and Al 7075 was decreased with an increase in temperature (Figure 6). Generally, the adsorption of organic molecules on metal surfaces cannot be considered as purely physical or chemical phenomenon, but the change in inhibition efficiency with temperature can be used to predict the predominant type of adsorption between inhibitor molecules and the metal surface. Adsorption of an inhibitor on the metal surface is responsible for impeding corrosion process by blockage of active surface sites.

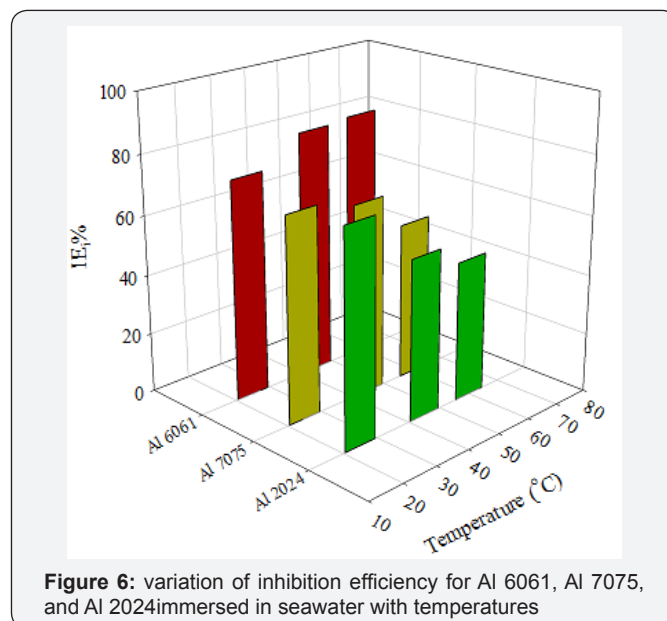


Figure 6: variation of inhibition efficiency for Al 6061, Al 7075, and Al 2024 immersed in seawater with temperatures

The adsorption may occur as a result of a weak interaction between the inhibitor molecules and the metal surface such as a weak Van der Waals or electrostatic forces; this is the general form of adsorption called physical adsorption. However, the stronger chemical adsorption occurs as a result of actual charge transfer or charge sharing between the inhibitor molecules and the metal surface [25]. In the case of physical adsorption, bonds are easily weakened by increasing temperature and partial desorption of the inhibitor molecules from the metal surface was achieved (adsorption/desorption equilibrium is shifted towards desorption) which reduced the surface coverage and reduced inhibition efficiency [31,32]. Thus, the predominant type of adsorption of the inhibitor on Al2024 and Al7075 surfaces might be due to weak physical adsorption than persistent chemical adsorption because the inhibition efficiencies decreased with increase in temperature. The opposite behavior may occur if the chemical adsorption is the predominant type of adsorption as in the case of Al 6061, in which inhibition efficiency increased with temperature.

Calculation of Activation Energy

Apparent activation energies (E_a) were evaluated from the effect of temperature on the corrosion current density in the absence and presence of an inhibitor using Arrhenius Eq.(3) to obtain more details on inhibition and corrosion process. Where,

T is the absolute temperature, K is the Arrhenius pre-exponential constant and R is the gas constant.

$$i_{corr} = K \exp\left(\frac{-E_a}{RT}\right) \quad (3)$$

Three cases were observed and reported in a previous study for the inhibitors based on the effect of temperature on the inhibition efficiency ($IE_i\%$) and apparent activation energy [33]:

a) $IE_i\%$ decreases with increase in temperature and

$$E_{a(\text{inhibition})} > E_{a(\text{free})}$$

b) $IE_i\%$ does not change with temperature and

$$E_{a(\text{inhibition})} = E_{a(\text{free})} \text{ and}$$

c) $IE_i\%$ Increases with temperature and

$$E_{a(\text{inhibition})} < E_{a(\text{free})}$$

Table 5: Activation energy (E_a kJ/mol) For Al 6061, Al 7075, and Al 2024 immersed in seawater without and with of specific concentration of LSAE.

Solution	E_a (KJ / mol)		
	Al 6061	Al 7075	Al 2024
Seawater	43.97	11.25	33.38
Seawater + inhibitor	33.04	19.98	48.35

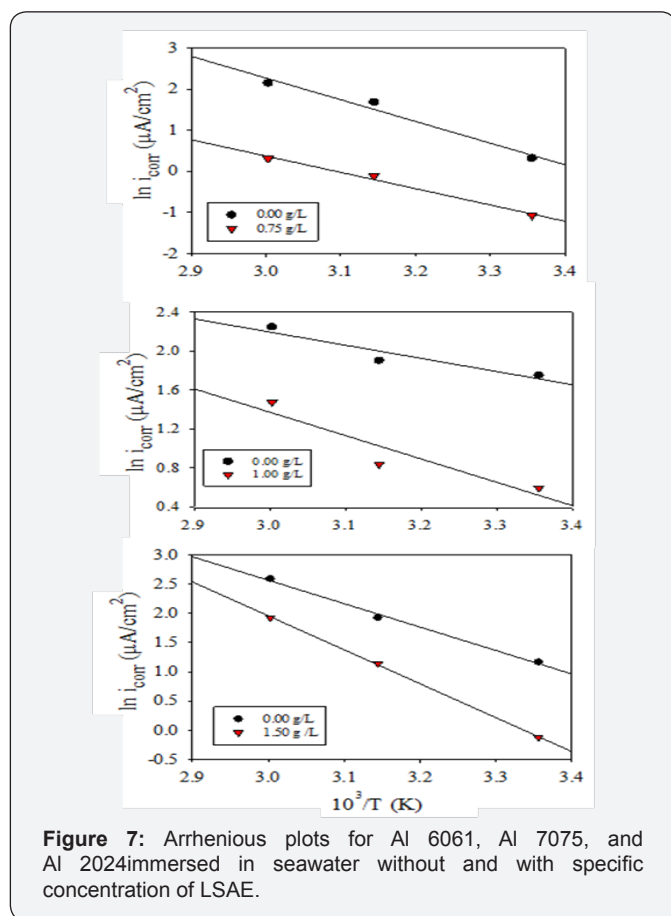


Figure 7: Arrhenius plots for Al 6061, Al 7075, and Al 2024 immersed in seawater without and with specific concentration of LSAE.

Activation energy values for the corrosion of the studied alloys without and with the inhibitor are listed in (Table 5) after they were estimated from the slopes ($-E_a/R$) of Arrhenius plots represented in (Figure 7). Al7075 with highest corrosion rate according to WL and PDP data (not shown here) showed the lowest activation energy (11.25 kJ/mole), while Al6061 had the highest energy barrier (43.97 kJ/mole) in the uninhibited solution. Activation energies of Al 2024 and Al 7075 in the presence of LSAE are greater than that in its absence and as their $IE_i\%$ decreased with temperature; they are in agreement with case 1.

The greater value of activation energy of the corrosion in the presence of an inhibitor as compared to the value of uninhibited solution is attributed to the physical adsorption. It can be explained as follows: if $IE_i\%$ decreases with increasing temperature, the adsorption process may become difficult and so, an increase in activation energy is expected [31-33] Conversely, adsorption of the inhibitor on Al6061 surface became better with increase in temperature as increased with temperature and activation energy of inhibited solution reduced as compared to the activation energy of the free solution. Inhibition of Al6061 is in agreement with case 3. Case 3 is explained by specific interaction between the metal surface and the inhibitor, and this is the main characteristic of chemisorptions [33]. Chemisorptions are also characterized by high heat of adsorption [25] which will be calculated and discussed in the next section.

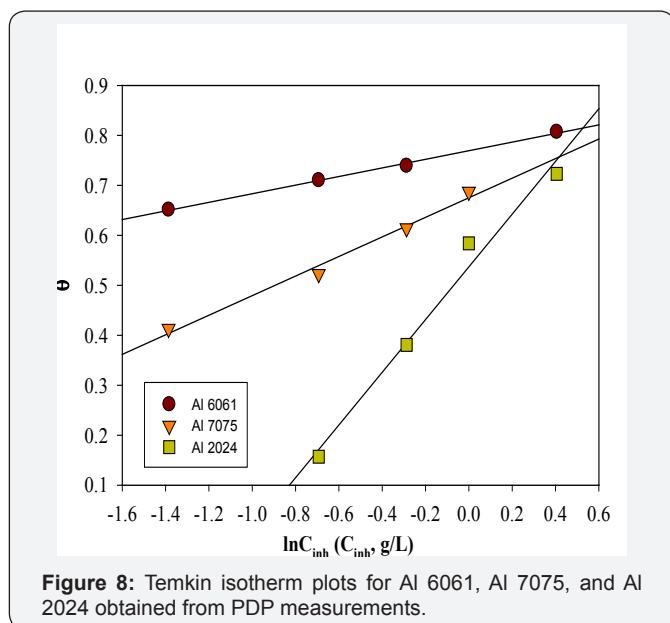
Adsorption Isotherm

Table 6: Thermodynamic parameters obtained from Temkin adsorption isotherm for aluminum alloys.

PDP measurements	Al 6061	Al 7075	Al 2024
$-\Delta G_{ads}$ (KJ / mol)	39.28	25.67	19.65
f	11.61	5.10	1.89
K_{ads} (Lg^{-1})	757.60	31.38	2.77
R^2	0.997	0.987	0.982

Adsorption is often described by isotherms, to get basic information on the interaction between the adsorbed molecules and the metal or alloy surface. Adsorption isotherms in corrosion inhibition researches relate the inhibitor concentration in the solution to the amount of inhibitor adsorbed by the surface coverage (θ) [4,25]. The surface coverage degree for various concentrations was determined by: ($\theta = (\frac{E_i\%}{100})$) and fitted into different adsorption isotherm models. According to the correlation coefficient values R^2 listed in (Table 6), Temkin adsorption isotherm given by Eq.(4) was found to be the best fit for the experimental polarization data for all the studied alloys, where f is the molecular interaction constant, θ is the surface coverage, K_{ads} is the adsorption equilibrium constant and C_{inh} is the inhibitor concentration.

$$\theta = f^{-1} \ln K_{ads} + f^{-1} \ln C_{inh} \quad (4)$$



Temkin isotherm takes into account heterogeneous nature of the surface and assumes a linear decrease in the heat of adsorption with surface coverage [25]. By plotting θ values versus $\ln C_{inh}$, straight lines were obtained (Figure 8) with the slopes equal to (f^{-1}) and their intercepts equal to $[f^{-1} \ln K_{ads}]$. The values of K_{ads} and f were calculated and listed in (Table 6) in addition to free energy of adsorption (ΔG_{ads}) which is related to the adsorption constant, K_{ads} by the Eq. (5), where C_{H_2O} is the water concentration, R is the universal gas constant and

T is temperature in Kelvin. Water concentration unit must be similar to the unit of the inhibitor.

$$\Delta G_{ads} = -RT \ln(K_{ads} \cdot C_{H_2O}) \quad (5)$$

Results in (Table 6) indicate that value K_{ads} of Al 6061 is quite different from that of Al7075 and Al 2024. Adsorption constant (K_{ads}) reveals the adsorption strength between the adsorbate (inhibitor molecules) and adsorbent (alloy surface). Higher value of K_{ads} implies better adsorption and higher inhibition efficiency. So, adsorption strength of the inhibitor molecules on the studied alloys surfaces follows the order: Al 6061 > Al7075 > Al 2024. This order is in agreement with WL results. In the work of [34], large difference also was reported between the adsorption constant values of aluminum and AA5754 inhibited by Laurel oil in acetic acid.

Values of ΔG_{ads} are negative for all the alloys. Negative sign proves the spontaneity of the adsorption process and the stability of the adsorbed layer [17]. ΔG_{ads} Of about -20 kJ/mole is consistent with physical adsorption mechanism. Thus, it is suggested that adsorption of the inhibitor on Al 2024 and Al 7075 was achieved mostly by physisorption mechanism. ΔG_{ads} Of Al 6061 is equal to -39.28 kJ/mole. It is close to the threshold value (-40 kJ/mole) required for the chemisorption [35]. So, it can be suggested that chemical adsorption is the major contributor to the adsorption mechanism in the case of Al 6061. The same result was also indicated after studying the effect of temperature on inhibition efficiency.

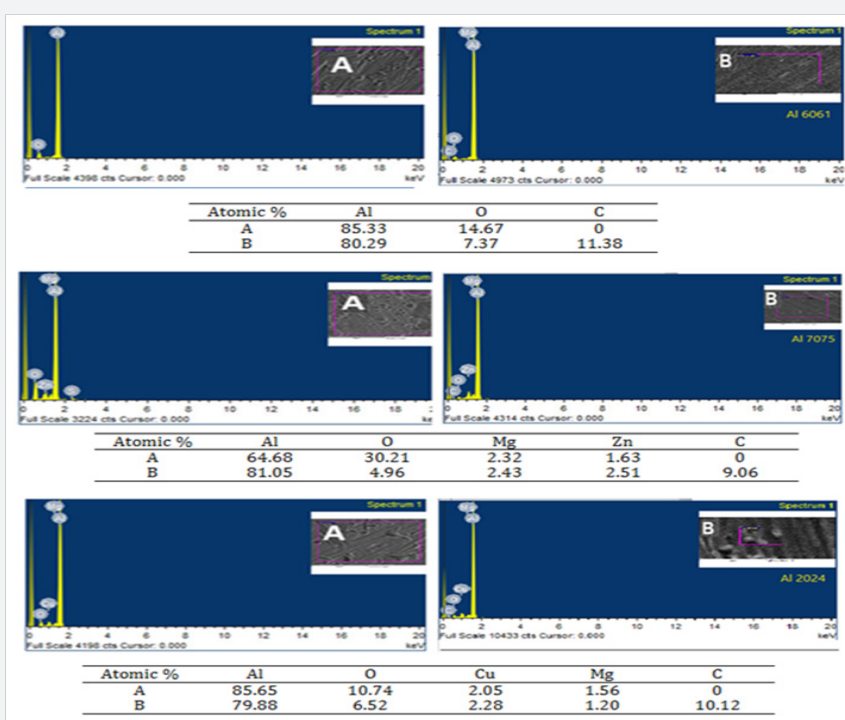


Figure 9: EDS analysis of Al 6061, Al 7075, and Al 2024 after immersed in seawater (A) without and (B) with specific concentration of LSAE (0.75 g/L) for 5 weeks.

Inhibition Mechanism

Corrosion inhibition is generally attributed to adsorption of the inhibitor molecules at the metal solution interface. PDP and WL results confirmed that addition of the LSAE to seawater effectively inhibited corrosion of aluminum alloys. ED's analysis was carried out to emphasize the adsorption of the inhibitor on aluminum alloys surfaces. (Figure 9) shows EDS analysis of Al 6061, Al 7075 and Al 2024 after they were immersed in seawater without and with the inhibitor for 5 weeks. The EDS analysis showed that the oxide percentage of the Al 6061, Al 7075 and Al 2024 surfaces exposed to seawater solution was 14.76%, 30.21, and 10.74, respectively.

However, the EDS analysis of the medium containing LSAE in seawater was 7.37, 4.96, and 6.52 %. The low oxygen percentage in seawater containing the inhibitor indicates that LSAE had an influence on the Al alloys surfaces, and thus inhibited the formation of aluminum oxide. This decrease in the quantity of oxygen could also be the result of anodic dissolution of the Al alloys through surface adsorption. These results led to the formation of a small amount of aluminum oxide. It was found also, In the presence of inhibitor, the spectra show an additional line, demonstrating the existence of C (owing to the carbon atoms of the LSAE). These data show that the carbonaceous material covered the Al alloys surfaces.

This layer is entirely owing to the inhibitor, because the carbon signal is absent on the specimens surfaces exposed to uninhibited seawater. Leek (*Allium ampeloprasum* var. Kurrat) seeds contain alkaloids, steroids, terpenoids, flavonoids, tannins, etc [36]. The presence of methiin and propiin, and sulphur containing bio-active constituents in *Allium* vegetables are mentioned in introduction. Because of the complex chemical composition of leek seeds, it is difficult to attribute the inhibition effect to a particular constituent. However, organic compounds interact with the metal surface or oxide-covered surface via hetero atoms with lone pair of electrons (as O, N and S) or by π -electrons. The inhibitor (leek seed powder) was analyzed by infrared spectroscopy to identify the functional groups present in it.

FT-IR spectrum of the powder is shown in a (Figure 10). The broad peak at 3413.44 cm^{-1} indicates the presence of strong hydroxyl group (O-H, stretching) and absorption at 2925.01 is due to sp^3 (C-H) stretching. The peak at 1637.38 cm^{-1} could be attributed to the stretching mode of (C=O) or (C=C) and the peak at 1074.76 is related to (C-O) stretching. The bands at 1402.16 and 656.36 cm^{-1} may be a result of bending vibration modes of (C-H) and (=C-H) bonds, respectively. The presence of O atom and unsaturated bonds meets the general characteristic of typical corrosion inhibitors [37]. Aluminum alloys immersed in seawater became covered with water molecules. Organic molecules were adsorbed on the Al alloys surfaces by replacing the water molecules according to Eq.(6), where n is the number of water molecules displaced by one inhibitor molecule, and n depends on the size and orientation of the inhibitor molecule [12].

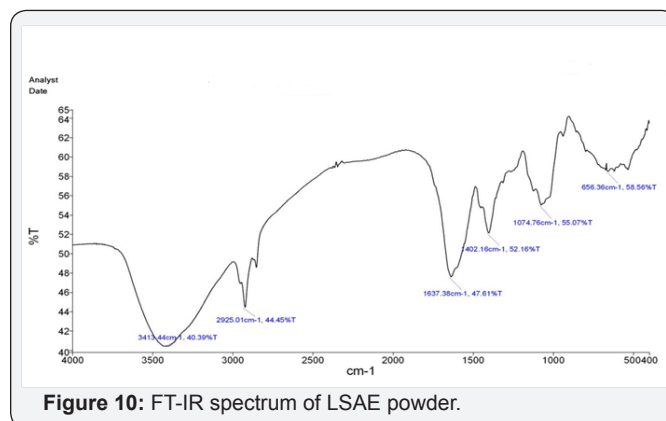
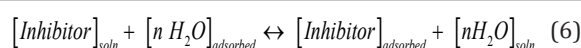


Figure 10: FT-IR spectrum of LSAE powder.



Strength of adsorption can be affected by several factors such as chemical structure of the inhibitor, temperature, nature as well as charge of the adsorbate-surface and the type of electrolyte [13]. The results show that the inhibitor was adsorbed strongly on Al 6061 surface as compared to the other alloy and Al 7075 adsorbed the inhibitor molecules better than Al 2024. Variation in surface microstructures of aluminum alloys is the reason for the difference in adsorption behavior. Adsorption strength was inversely proportional to the availability of Cu-rich intermetallic particles in Al alloys surface.

Conclusion

- Al 6061 showed the highest inhibition efficiency and adsorption strength followed by Al 7075 and then Al 2024. This order is contrary to the numbers of cathodic Cu-containing IM particles present on the alloys surfaces.
- The inhibition efficiency of Al 2024 and Al 7075 was decreased with an increase in temperature which may be attributed to the physical adsorption rather than chemical but the inhibition efficiency of Al 6061 increased with temperature. Thus chemical adsorption is the predominant type of adsorption in case of Al 6061.
- The adsorption of LSAE on alloys surfaces in seawater fitted Temkin adsorption isotherm and the negative values of free energy revealed the spontaneous nature of the adsorption process.

References

- I Polmear (2006) *Light Alloys: From Traditional Alloys to Nanocrystals*. (4th edn), Butterworth-Heinemann, Oxford, UK pp. 1-27.
- V Zolotarevskii, N Belov, M Glazoff (2007) *Casting Aluminum Alloys*. UK, pp. 1-90.
- JR Davis (1999) *Corrosion of Aluminum and Aluminum Alloys*. ASM International, US pp. 1-250.
- D Landolt (2007) *Corrosion and Surface Chemistry of Metals*. CRC Press, US pp. 1-627.
- Z S zklarska Smialowska (1999) *Pitting Corrosion of Aluminum* *Corros Sci* 41: 1743-1767.
- DA Shifler, T Tsuru, PM Natishan, S Ito (2005) *Corrosion in Marine and*

- Saltwater Environment II. The Electrochemical Society, US pp. 173-256.
7. KA Chandler (2014) Marine and Offshore Corrosion: Marine Engineering Series. UK pp. 116-140.
 8. KS Rao, KP Rao, Trans (2004) Pitting Corrosion of Heat-Treatable Aluminium Alloys and Welds: a review. Indian Inst Met 57(6): 593-610.
 9. IW Huang, BL Hurley, F Yang, RG Buchheit (2016) Dependence on Temperature, pH, and Cl⁻ in the Uniform Corrosion of Aluminum Alloys 2024-T3, 6061-T6, and 7075-T6. Electrochim Acta 199: 242-253.
 10. RM Palou, O Olivares Xomelt, NV Likhanova, in: M. Aliofkhaezrai Eds. (2014) Developments in Corrosion Protection. InTech pp. 431-465.
 11. CG Darvia, GF Alexandre, M Aliofkhaezrai (2014) Developments in Corrosion Protection. InTech pp. 365-379.
 12. S Papavinasam, RW Revie (2000) Uhlig's Corrosion Handbook. John Wiley & Sons, Canada pp. 1021-1046.
 13. H Gerengi (2012) Anticorrosive Properties of Date Palm (Phoenix dactylifera L) Fruit Juice on 7075 Type Aluminum Alloy in 3.5% NaCl Solution. Ind Eng Chem Res 51(39): 12835-12843.
 14. VS Sastri (2011) Green Corrosion Inhibitors : Theory and Practice. John Wiley & Sons, US pp. 1-257.
 15. OS Olanrewaju, AH Saharuddin, AS Ab Kader, WMN Wan Nik (2014) Marine Technology and Sustainable Development. IGI Global, US pp. 146-156.
 16. SK Sharma (2011) Green Corrosion Chemistry and Engineering: Opportunities and Challenges. Wiley-VCH, Germany pp. 4-22.
 17. A Singh, Y Lin, W Liu, Sn Yu, J Pan, et al. (2014) Plant Derived Cationic Dye as an Effective Corrosion Inhibitor For 7075 Aluminum Alloy in 3.5% NaCl Solution. J Ind Eng Chem 20(6): 4276-4285.
 18. R Rosliza, S Izman (2011) SEM-EDS Characterization of Natural Products on Corrosion Inhibition of Al-Mg-Si alloy. Prot Met.Phys Chem.Surfaces 47(3): 395-401.
 19. Y Mohamed Yasseen, SA Barringer, WE Splittstoesser (1995) In Vitro Shoot Proliferation and Plant Regeneration From Kurrat (Allium ampeloprasum var. Kurrat) Seedlings. Plant Cell, Tissue Organ Cult 40 (2): 195-196.
 20. P Dey, KL Khaled (2015) An Extensive Review on Allium ampeloprasum: A magical Herb. Int J Sci Res 4(7): 371-377.
 21. AH Al Moubaraki, A Al Judaibi, M Asiri (2015) Corrosion of C-steel in the Red Sea: Effect of Immersion Time and Inhibitor Concentration. Int J Electrochem Sci 10: 4252-4278.
 22. (2011) ASTM G1-03 (2011) Standard Practice for Preparing, Cleaning, and Evaluating Corrosion Test Specimens.
 23. HS Khatak, B Raj (2002) Corrosion of Austenitic Stainless Steels : Mechanism, Mitigation and Monitoring. Elsevier Science, UK p. 40.
 24. R Baboian (2005) Corrosion Tests and Standards. ASTM international, US pp. 109-130.
 25. E Mc Cafferty (2010) Introduction to Corrosion Science. US pp. 1-427.
 26. (1980) Basic of corrosion measurement. Princet Appl Res.
 27. AFrignani, G Trabanelli, F Zucchi (1975) Proceedings 4th European Symposium on Corrosion Inhibitors. Ann Univ Ferrara, Italy p. 652.
 28. TP Hoar, RP Khera (1961) Comptes Rendus du Symposium European sur les Inhibit de Corros. Ann Univ Ferrara, Italy p. 73.
 29. R Rosliza, A Nora'aini, WB Wan Nik (2010) Study on the Effect of Vanillin on the Corrosion Inhibition of Aluminum Alloy. J Appl Electrochem 40(4): 833-840.
 30. L Niu, YF Cheng (2009) Cathodic Reaction Kinetics and Its Implication on Flow-Assisted Corrosion of Aluminum Alloy in Aqueous Ethylene Glycol Solution. J Appl Electrochem 39(8): 1267-1272.
 31. SK Shukla , EE Ebenso (2011) Corrosion Inhibition, Adsorption Behavior and Thermodynamic Properties of Streptomycin on Mild steel in Hydrochloric Acid Medium. Int J Electrochem Sci 6(8): 3277-3291.
 32. M Lebrini, F Robert, C Roos (2010) Inhibition Effect of Alkaloids Extract From Annona Squamosa Plant on the Corrosion of C38 Steel in Normal Hydrochloric Acid Medium. Int J Electrochem Sci 5 (11) 1698-1712.
 33. A Popova, E Sokolova, S Raicheva, M Christov (2003) AC and DC Study of the Temperature Effect on Mild Steel Corrosion in Acid Media in the Presence of Benzimidazole Derivatives. Corros Sci 45(1) 33-58.
 34. J Halambek, MC Bubalo, IR Redovnikovic, K Berkovic (2014) Corrosion Behaviour of Aluminium and AA5754 Alloy in 1% Acetic Acid Solution in Presence of Laurel Oil. Int J Electrochem Sci 9(10): 5496-5506.
 35. L Olanrekanmi, IB Obot, MM Kabanda, EE Ebenso (2015) Some Quinoxalin-6-yl Derivatives as Corrosion Inhibitors For Mild Steel in Hydrochloric Acid: Experimental and Theoretical Studies. J Phys Chem C 119(28): 16004-16019.
 36. FA Abd El Rehem, RF Ali (2013) Proximate Compositions, Phytochemical Constituents, Antioxidant Activities and Phenolic Contents of Seed and Leaves Extracts of Egyptian Leek (Allium ampeloprasum var. Kurrat). Eur J Chem 4(3): 185-190.
 37. KK Alaneme, SJ Olusegun, OT Adelowo (2016) Corrosion Inhibition and Adsorption Mechanism Studies of Hunteria Umbellata Seed Husk Extracts on Mild Steel Immersed in Acidic Solutions, Alexandria Eng J 55(1): 673-681.



This work is licensed under Creative Commons Attribution 4.0 License
 doi: 10.19080/OMCIJ.2017.03.555624

**Your next submission with Juniper Publishers
 will reach you the below assets**

- Quality Editorial service
- Swift Peer Review
- Reprints availability
- E-prints Service
- Manuscript Podcast for convenient understanding
- Global attainment for your research
- Manuscript accessibility in different formats
(Pdf, E-pub, Full Text, Audio)
- Unceasing customer service

Track the below URL for one-step submission

<https://juniperpublishers.com/online-submission.php>